Carbohydrate Polymers 86 (2011) 1790–1798

Contents lists available at ScienceDirect

Carbohydrate Polymers

journal homepage: www.elsevier.com/locate/carbpol

Cellulose nanocomposites with nanofibres isolated from pineapple leaf fibers for medical applications

Bibin Mathew Cherian[a,*], Alcides Lopes Leão[a,*], Sivoney Ferreira de Souza[b], Ligia Maria Manzine Costa[b], Gabriel Molina de Olyveira[b], M. Kottaisamy[c], E.R. Nagarajan[d], Sabu Thomas[e]

[a] Department of Natural Resources, São Paulo State University (UNESP), Botucatu 18610-307, São Paulo, Brazil
[b] Department of Nanoscience and Advanced Materials, Universidade Federal do ABC (UFABC) Santo André 09210-170, São Paulo, Brazil
[c] Department of Chemistry, Thiagarajar College of Engineering, Madurai 625 015, Tamil Nadu, India
[d] Centre for Nanotechnology, Kalasalingam University, Anand Nagar, Krishnankoil 626 190, Virudhunagar, Tamil Nadu, India
[e] Centre for Nanoscience and Nanotechnology, Mahatma Gandhi University, Kottayam 686 560, Kerala, India

ARTICLE INFO

Article history:
Received 13 February 2011
Received in revised form 1 July 2011
Accepted 10 July 2011
Available online 19 July 2011

Keywords:
Pineapple leaf fibre (PALF)
Cellulose Nanofibres
Polyurethane
Nanocomposites
Medical application

ABSTRACT

Nanocellulose is the crystalline domains obtained from renewable cellulosic sources, used to increase mechanical properties and biodegrability in polymer composites. This work has been to study how high pressure defibrillation and chemical purification affect the PALF fibre morphology from micro to nanoscale. Microscopy techniques and X-ray diffraction were used to study the structure and properties of the prepared nanofibers and composites. Microscopy studies showed that the used individualization processes lead to a unique morphology of interconnected web-like structure of PALF fibers. The produced nanofibers were bundles of cellulose fibers of widths ranging between 5 and 15 nm and estimated lengths of several micrometers. Percentage yield and aspect ratio of the nanofiber obtained by this technique is found to be very high in comparison with other conventional methods. The nanocomposites were prepared by means of compression moulding, by stacking the nanocellulose fibre mats between polyurethane films. The results showed that the nanofibrils reinforced the polyurethane efficiently. The addition of 5 wt% of cellulose nanofibrils to PU increased the strength nearly 300% and the stiffness by 2600%. The developed composites were utilized to fabricate various versatile medical implants.

1. Introduction

Research for development of biodegradable materials from renewable sources is increasing. The availability of biopolymers, relatively cheaper, which occur in abundance in nature, can be cited as an important reason. An example of biopolymers presenting these advantages is cellulose. The recent interest in using stiff nanometric particles as reinforcement materials in polymeric matrixes, composites or nanocomposites, has been increasing. Two good examples of these types of particles are carbon nanotubes and cellulose nanocrystals. Cellulose nanocrystals, also reported in the literature as whiskers, nanofibers, cellulose crystallites or crystals, are the crystalline domains of cellulosic fibers, isolated by means of acid hydrolysis, and are called in this way due to their physical characteristics of stiffness, thickness, and length (De Souza Lima & Borsali, 2004).

Samir, Alloin, and Dufresne (2005) report that cellulose whiskers are regions growing under controlled conditions, which allows individual high-purity crystals to form. Their highly ordered structure may not only impart high resistance, but also make significant changes to some important properties of materials, such as electrical, optical, magnetic, ferromagnetic, and dielectric nature, as well as concerning conductivity.

Since cellulose is classed as a carbohydrate (a substance containing carbon, hydrogen and oxygen), it is necessary to point out that although this term applies to a large number of organic compounds, cellulose is unique in that it can be either synthesized from, or hydrolyzed to, monosaccharides (Khadem, 1988). The repeating unit of the cellulose polymer is known to comprise two anhydroglucose rings joined via a β-1,4 glycosidic linkage from

Abbreviations: PALF, Pineapple leaf; NC, Nanocellulose; PU, Polyurethane; min, Minutes; DP, Degree of polymerization; BC, Bacterial cellulose; NaOH, Sodium hydroxide; CH_3COOH, Acetic acid; NaClO, Sodium hypochlorite; $H_2C_2O_4$, Oxalic acid; MDI, Methylene di-*p*-phenyl-diisocyanate; BD, 1,4-Butanediol; MIDE, 2,2′-(Methylimino)diethanol; DMF, *N*,*N*-dimethylformamide; PCL-diol, Polycaprolactone diol; M_n, Molecular weight; kPa, Kilopascal; MPa, Megapascal; rpm, Revolutions per minute; XRD, X-ray diffraction; SEM, Scanning Electron Microscopy; ESEM, Environmental Scanning Electron Microscopy; AFM, Atomic Force Microscopy; A_0, Free amplitude; r_{sp}, Set-point ratio; A_{sp}, Setpoint amplitude; THF, Tetrahydrofuran; PTFE, Polytetrafluoroethylene; mm, Millimetre; μm, Micrometre; nm, Nanometre.

* Corresponding authors. Tel.: +55 14 3811 7162/7163; fax: +55 14 3811 7202.
E-mail addresses: bmcherian@gmail.com (B.M. Cherian), alcidesleao@fca.unesp.br (A.L. Leão).

0144-8617/$ – see front matter © 2011 Elsevier Ltd. All rights reserved.
doi:10.1016/j.carbpol.2011.07.009

this unit (called cellobiose) (Klemm, Philipp, Heinze, Heinze, & Wagenknecht, 1998).

In its native form cellulose is typically called cellulose-I. This cellulose-I crystal form, or native cellulose, also comprises two allomorphs, namely cellulose Iα and Iβ (Atalla & Vanderhart, 1984). The ratio of these allomorphs is found to vary from plant species to species, but bacterial and tunicate forms are Iα and Iβ rich, respectively. The crystal structures of cellulose allomorphs Iα and Iβ have been determined with great accuracy, particularly the complex hydrogen bonding system (Nishiyama, Langan, & Chanzy, 2002; Nishiyama, Sugiyama, Chanzy, & Langan, 2003). The hydrogen bond network makes cellulose a relatively stable polymer, which does not readily dissolve in typical aqueous solvents and has no melting point. This network also gives the cellulose chains a high axial stiffness (Kroonbatenburg, Kroon, & Northolt, 1986).

Generally, cellulose-based biofibers, counting PALF, banana, cotton, flax, hemp, jute and sisal, and wood fibers are used to reinforce plastics due to their relative high-strength, high stiffness and low density (Alves et al., 2010; Arib, Sapuan, Ahmad, Paridah, & Zaman, 2006; Jacob, Francis, Varughese, & Thomas, 2006; Jacob, Varughese, & Thomas, 2006; John & Anandjiwala, 2009; Kim, Moon, Kim, & Ha, 2008; Placet, 2009; Pothan, Cherian, Anandakutty, & Thomas, 2007). Because of their annual renewability, agricultural crops-residues can be a valuable source of natural fibers. Biocomposites have future commercial application that would unlock the potential of these underutilized renewable materials and provide a non-food based market for agricultural industry (John & Thomas, 2008). In addition, they are biodegradable and offer potential advantages over unmanageable synthetic plastics in disposable applications (Jacob, Jose, Jose, Varughese, & Thomas, 2010; John, Anandjiwala, Pothan, & Thomas, 2007). Recent advances in producing bio-fibers, microfibrillated or nano-size fibers with the high-strength and surface area offer manufacturing high-performance composites from these bio-fibers (Chakraborty et al., 2006; Dufresne & Vignon, 1998; Nakagaito & Yano, 2005).

The reinforcing cellulosic nanofibers obtained from PALF fibers used for the preparation of nanocomposites are developed by the process of steam treatment correlated with acid treatment. Steam treatment is a hydrothermal process of biomass treatment, involving the application of steam at high pressure, and, which can be performed by batch or continuous reactor. The biomass is exposed to saturated steam (180–230 °C) for 20–40 min; during this time, hemicellulose is hydrolysed and solubilized. Pressure is then suddenly lowered to the atmospheric value. In doing so, the biomass undergoes an explosive decompression which induces disruption of the plant cells. Among the alternative separation processes for biomass components, the research team adopted steam treatment due to its attractiveness. The attractive features of steam treatment in comparison to autohydrolysis, pulping and other methods include the potential for significantly reducing the environmental impact, the investment costs and the energy consumption. Furthermore, less hazardous chemicals are used and a more complete recovery of all plant biopolymers in a useful form is possible (Avellar & Glasser, 1998). Generally, the steaming process results in a hydrolysis of glycosidic bonds in the hemicelluloses and, to a lesser extent in the cellulose. It also leads to a cleavage of hemicellulose–lignin bonds. The reactions result in an increased water solubilization of hemicelluloses and in an increased solubility of lignin in alkaline or organic solvents, leaving the cellulose as a solid residue with a reduced degree of polymerization (DP). PALF fibre bundles were employed for the production of nanofibrils, which at present is the waste product of pineapple cultivation. Tones of unused PALF fibre residues are generated every year, with only a small percentage being used in applications such as feedstock and energy production. The development of biocomposites has increased commercial application that would unlock the potential of these underutilized renewable materials and provide a non-food based market for agricultural industry.

Pineapple leaf fibre (PALF) is an important natural fibre that exhibits high specific strength and stiffness. The fibers have a ribbon-like structure and consist of a vascular bundle system present in the form of bunches of fibrous cells, which are obtained after mechanical removal of all the epidermal tissues. PALF is of fine quality, and its structure is without mesh and can be extracted into nanofibers thinner than fibers from bacterial cellulose (BC) and tunicates. The fibre is very hygroscopic, relatively inexpensive and abundantly available. The PALF observed to have the high percentage of α-cellulose content (81.27%) and low percentage of hemicellulose (12.31%) and lignin (3.46%) content (Cherian et al., 2010). The α-cellulose is purified with steam treatment correlated with acid treatment processes. The superior mechanical properties of PALF are associated with its high α-cellulose content and comparatively low microfibrillar angle (14°). Due to the unique properties exhibited by pineapple leaf fibre (PALF) they can be used as excellent potential reinforcement in composite matrices (Lopattananon, Panawarangkul, Sahakaro, & Ellis, 2006).

The cellulose or wood polymer composites always face the interfacial problem due to the cellulose being hydrophilic and polar and the polyolefins being hydrophobic (Bengtsson, Gatenholm, & Oksman, 2005). In this study hydrophilic polyurethane has been used as the matrix polymer. When the polyurethane is used as matrix, it is believed that no adhesion problem would occur and the dispersion would be much better.

Polyurethanes are an interesting family of polymers which have been used in many different applications such as biomedical, coatings, adhesives and composites (Gorrasi, Tortora, & Vittoria, 2005; Moon, Kim, Nah, & Lee, 2004). Polyurethanes form a copolymer structure with the isocyanates as hard domains and polyols as soft domains. The properties of the polyurethanes can be adjusted mainly by two routes. The first route is based on the chemistry of polyurethanes formulating the polyurethane based on different isocyanate/polyol ratio and using different amounts of chain extender. The second route is altering the properties of the polyurethanes with different fillers and reinforcements (Gorrasi et al., 2005). Polyurethanes have been reinforced with certain fillers such as talc, mica and glass fibre in the form of polymer matrix composite material (Gorrasi et al., 2005). These materials increase the tensile strength but decrease the elongation to break and discolour the polymer (Sternitzke, Derby, & Brook, 1998; Vaia, 2002). The aim of this study was to examine the effect of fibrillation of cellulose fibers from PALF using a high pressure steam treatment and investigate the reinforcing effect of nano sized cellulose fibrils in the polyurethane matrix especially for medical implants. Earlier studies made on polyurethane and cellulose both as micro and nanocomposites have been reported by Auad, Contos, Nutt, Aranguren, and Marcovich (2005) and Rials, Wolcott, and Nassar (2001) but high crystalline nanofibrils of PALF prepared by steam explosion process, reinforced in a polyurethane matrix particularly used for medical application has not been reported before.

2. Experimental

2.1. Materials

The materials used for the study includes PALF fibers were supplied by the company Superpolpa from Iaras – SP, Brazil, Sodium hydroxide (NaOH), Acetic acid (CH_3COOH), Sodium hypochlorite (NaClO) and Oxalic acid ($H_2C_2O_4$) of analytical purity grade were purchased from Merck and Co., Inc., Methylene di-*p*-phenyl-diisocyanate (MDI, 99%, Sigma–Aldrich), 1,4-butanediol (BD, 99%, Sigma–Aldrich), 2,2′-(methylimino)diethanol (MIDE,

99%, Sigma–Aldrich), and *N*,*N*-dimethylformamide (DMF, 99%, Sigma–Aldrich) and polycaprolactone diol (PCL-diol) with M_n = 530 were used as received. MDI was purified through vacuum distillation, while BD was distilled with calcium hydrogen in a vacuum to eliminate moisture. DMF was distilled over calcium hydrogen at the atmospheric pressure under nitrogen protection. MDI was chosen because it is widely used in synthesis of biomedical polyurethanes due to its reactivity and PCL-diol was chosen because of its biodegradability.

2.2. Isolation of cellulose nanofibrils

PALF fibers were treated with 2% NaOH (fibre to liquor ratio 1:10) in an autoclave and kept under 138 kPa pressure for a further period of 1 h. Pressure was released immediately. The fibers were removed from the autoclave, and the fibers were washed in distilled water until it was rid of alkali. The steam exploded fibers (87% yield) were bleached using a mixture of NaOH and glacial CH_3COOH (27 g/L and 78.8 g/L respectively) and a mixture of 1:3 NaClO solutions. The bleaching was repeated six times. After the bleaching the fibers were thoroughly washed in distilled water and dried. The steam exploded bleached fibers (76% yield) were treated with $H_2C_2O_4$ of 11% concentration in an autoclave until it attained a pressure of 138 kPa. The pressure was released immediately. The autoclave was again set to reach 138 kPa and the fibers were kept under that pressure for 15 min. The pressure was released and the process repeated eight times. The fibers were taken out washed until the washings no longer decolorized $KMnO_4$ solution to make sure that the washings are free from acid. The proceeded nanofibrils (69% yield) were suspended in distilled water and kept stirring with a mechanical stirrer of type RQ-1.27 A and 8000 rpm for about 4 h until the fibers are dispersed uniformly.

2.3. Characterization of fibers

2.3.1. X-ray diffraction (XRD)

Wide-angle X-ray diffraction data were collected using a Rigaku 200B X-ray diffractometer (40 kV, 40 mA) equipped with Cu Kα radiation (λ = 0.1541 nm). Patterns were recorded by monitoring diffractions from 1.5° to 30°. The scan speed was 2°/min.

2.3.2. Scanning Electron Microscopy (SEM) analysis

Scanning electron micrographs of treated and untreated fibers and composites were captured using Philips SEM 515. In this case, the samples were coated with platinum using the sputtering technique.

2.3.3. Environmental Scanning Electron Microscopy (ESEM) analysis

Philips XL30 FEG ESEM was also used to observe the morphology of dried nano film with an accelerating voltage of 30 kV. The nanofibers were analyzed using water suspension of the nanofibers. A drop of suspension of nanofibers was kept onto a carbon film and left to dry in a silica gel ambient for 12 h followed by coating with platinum using the sputtering techniques. The film was sputter-coated with platinum using a Baltec SCD050 sputter coater for enhanced conductivity.

2.3.4. Atomic Force Microscopy (AFM) analysis

Cellulose nanofibrils were observed using atomic force microscopy, NanoScope IVa, Multimode SPM (Veeco Inc. Santa Barbara, USA), in tapping mode. Calibration was performed by scanning a calibration grid with precisely known dimensions. All scans were performed in the air with commercial Si Nanoprobes SPM tips with a resonance frequency of about 300–330 kHz. A free amplitude (A_0) of about 20 nm and a set-point ratio (r_{sp}) between 0.4 and 0.6 were used. r_{sp} is the ratio between the setpoint amplitude (A_{sp}) and A_0. Image processing, including flattening was made. Height and phase images were obtained simultaneously in tapping mode at the fundamental resonance frequency of the cantilever with a scan rate of 0.5 line/s using a j-type scanner. The free oscillating amplitude was 3.0 V, while the set point amplitude was chosen individually for each sample. For each sample image was scanned on at least five different fibers. Usually two different areas of each fibre were investigated. Only one representative image of sample is shown. Samples of cellulose nanofibril for characterization were prepared by pipetting a 0.12 g/L aqueous whisker suspension was allowed to dry on a freshly cleaved mica surface. The sample was allowed to dry in room temperature overnight.

2.4. Preparation of nanocomposites

The preparation of polyurethane–cellulose nanocomposite is as follows.

2.4.1. Synthesis of degradable PUs

Degradable PUs were synthesized using a two-step method. The stoichiometry of the PU synthesis reaction was approximately 2:1:1 of hard segment (diisocyanate)/soft segment (PCL-diol)/chain extender (1,4-BD). The MDI was dissolved in 50 mL DMF and PCL-diol were added drop wise into the MDI solution. This mixture was allowed to react at 60 °C for a period of 3 h. The solution was cooled to 25 °C, 100 mL DMF was added, and then 5% (w/v) chain extender in DMF was added drop wise to the reaction mixture and stirred for 18 h. After the reaction was finished, the polymer solution was precipitated in distilled water, and dried in a vacuum oven at 60 °C for at least 48 h before further use and characterization.

2.4.2. Preparation of PU films

Polymer films were prepared by solvent casting. The synthesized PUs were dissolved in tetrahydrofuran (THF) at a concentration of 4% (w/v). Polymer solution (12 mL) was then poured into levelled 5 cm PTFE casting plates and cast into thick films at room temperature. Casting plates were covered to prevent dust from contaminating the films and excessive fast casting, which may induce bubbles and result in surface defects. The cast films were removed from the casting plates and dried in a vacuum oven at 60 °C for 4 h to remove residual solvent. The average thickness of the film was about 0.08–0.10 mm.

2.4.3. Preparation of nonwoven nanofibril mats

The nonwoven mats of cellulose fibers and nanofibrils were formed by filtering the water–nanocellulose slurry. For the nanocellulose, special membrane filter (polyethersulfone, 0.1 μm) was used for mat formation of fibrils was used for drying and forming the mat. The slurry was agitated during the filtering process to distribute the nanocellulose evenly on the mesh. The nanocellulose formed mat could easily be peeled off from the mesh after drying due to strong hydrogen bonds. The thickness of the fibre mat was adjusted by altering the cellulose concentrations on the water–nanocellulose slurry. The thickness of the mats varied between 0.05 and 0.2 μm.

2.4.4. Nanocomposite preparation

The composite materials were prepared by the film-stacking method. In this method, the PU films and non woven nanocellulose mats were stacked and compression moulded. The temperature (150–200 °C), pressure (10,000–20,000 kPa) and compression time (1–4 min) were varied to find the optimum composite properties. The compression moulding conditions were optimized to 175 °C at 10,000 kPa for 1 min and 30 s. The final composites were prepared

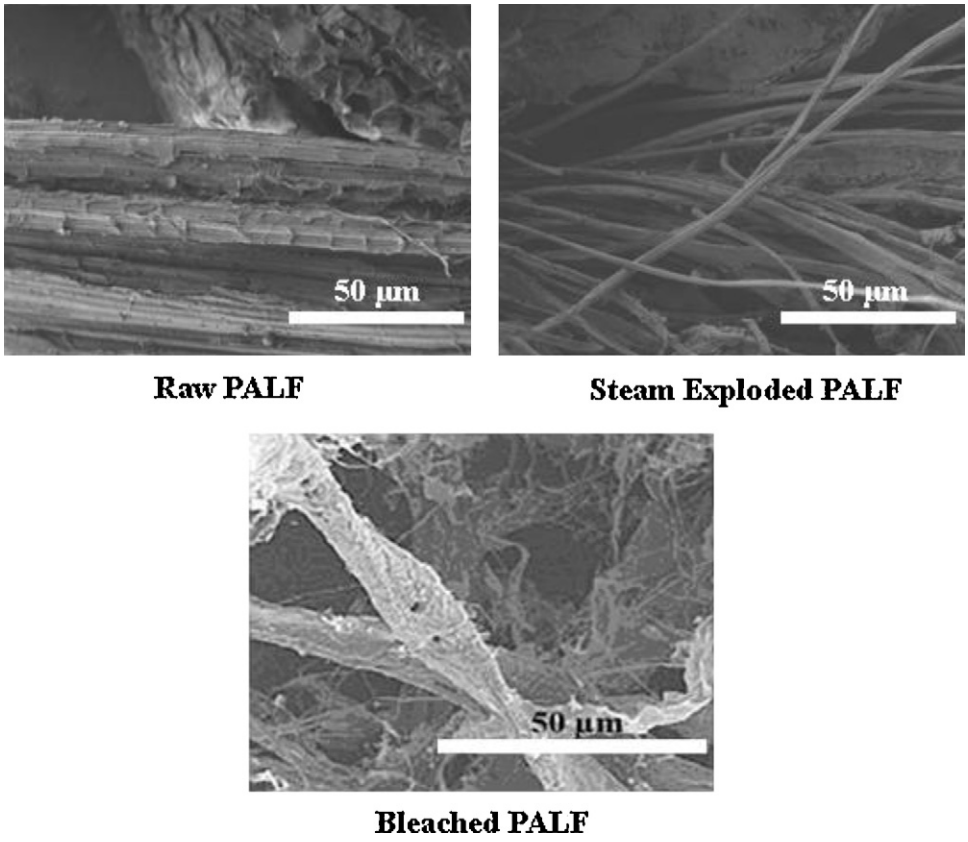

Fig. 1. SEM micrographs of raw, steam exploded and bleached PALF fibers.

with nanocellulose loadings of 2 [PU–NC(2%)], 5 [PU–NC(5%)] and 10 [PU–NC(10%)] percentage.

The medical implants were fabricated in desired moulds using non woven nanocellulose mats and PU film with nanocellulose loading of 5% with processing temperature of 175 °C at 10,000 kPa for 1 min and 30 s.

2.5. Mechanical test

Tensile properties of the neat polymer and composite materials were measured using Tensile Testing Machine (Zwick Z 250) following DIN EN 52. Test was performed until tensile failure occurred. The measurements were done at 25 °C. Samples dimensions were 0.1 mm × 5 mm × 50 mm. The maximum strength was obtained from the stress–strain curves. Ten specimens were tested and at least five replicate specimens were presented as an average of tested specimens.

3. Results and discussion

3.1. Scanning Electron Microscopical analysis

In order to further investigate the structural changes in the fibers, SEM pictures of the PALF fibers were taken and are shown in Fig. 1. These pictures visually suggest the partial removal of hemicelluloses, lignin and pectin after high pressure chemical treatment, which are the cementing materials around the fibre bundles. It is clear from the micrograph that the average diameter of the fibers is about 10–15 μm, which is lower than the average size of the fibre bundle, 50–125 μm before steam treatment.

Fig. 1 shows the structure and appearance of PALF fibers in macro to micro-scale by SEM. It can be seen from the SEM images that small fibrils with the diameter less than 1 μm were projected from the surface of raw fibre when the fibre undergoes steam treatment at high pressure. It is clear from the SEM micrographs that high pressure steam treatment helps in fibre separation and fibrillation. The tendency for fibre defibrillation is found to increase with high pressure steaming coupled with acid treatment. These conclusions are further supported by the ESEM images shown in Fig. 2. It is well evident from the ESEM images that fibrillation trends increased along with the acid treatment and high pressure drop. The drop in pressure facilitates the increase in the fibrillation process of the PALF fibers whose size ranges in nanometres.

It can be seen from ESEM image shown in Fig. 2 that the cellulose nanofibres obtained from the PALF fibers are in the

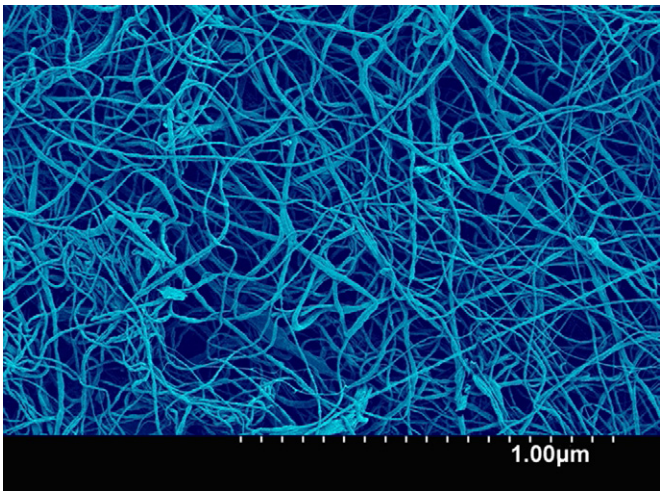

Fig. 2. ESEM image of acid treated PALF fibre.

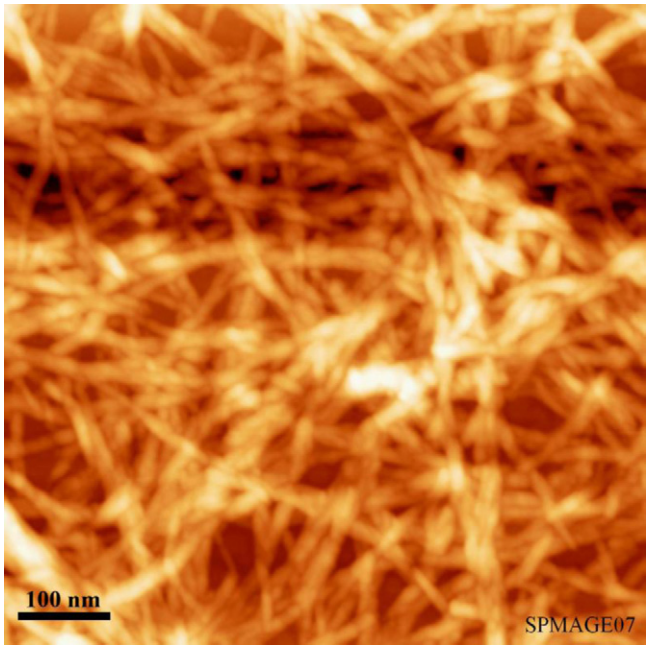

Fig. 3. AFM micrographs of acid treated PALF fibre.

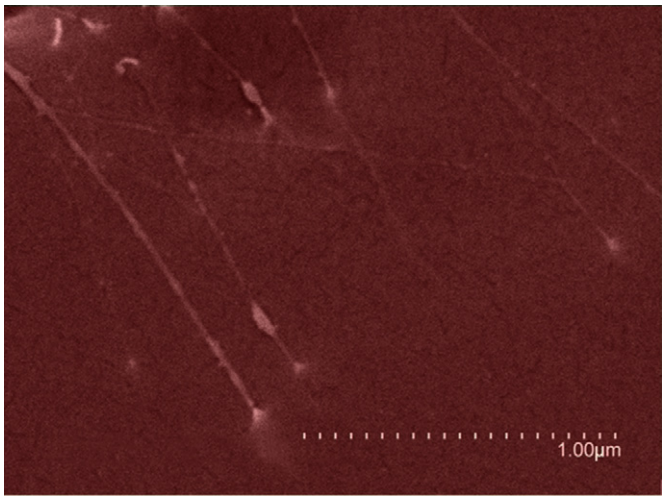

Fig. 4. ESEM image of polyurethane–nanocellulose (5%) nanocomposite.

entangled fibril form and the length to diameter ratios are in the range of 1 μm to 15 nm, having a wide range of aspect ratio (length/diameter), the average value being 67. It is possible to see that most of the nanofibrils are agglomerates of hundreds of individual cellulose nanocrystals whose aspect ratios (≈67) are appropriate for efficient reinforcement in polymeric matrices. This is due to the fact that reinforcements are nanosized, the large aspect ratio (length/diameter) could make the composite behave like a continuous fibre composite. Because of their small sizes, these nanostructured materials have high surface to volume ratios, which affect not only the functional properties but also enhance the mechanical properties such as the elastic modulus of these nanofibrils reinforced nanocomposites.

The produced nanofibrils seem to be in the form of well interconnected web like structure having the suitable aspect ratio for reinforcing in polymeric matrices. From the pineapple leaf, PALF fibers are extracted by mechanical methods. As it was previously mentioned, these fibers have diameters in the micron range. After the steam treatment conducted for the partial removal of different fibre components, a decrease in fibre diameter, by separating the micro fibrils (87% yield) as well as a change in the fibre's composition has been found to occur (cellulose purification). The chemical bleaching process separates out the highly purified cellulose microfibrils (76% yield). Elementary nanofibres obtained after acid coupled steam treatment (69% yield) showed a helicoidal ribbon-shaped structure (related to cellulose ordered chains) that appears evident after the total extraction procedure. It is possible that these fibers were formed by nano-ordered chains that can be separated by steam coupled acid treatment. Thus the high pressure steaming paved way for the splitting of nanofibrils of PALF fibers and increased the surface area of the fibers which helps to maximise the reinforcement ability in polymeric matrices.

The surface morphology of the nanofibrils surface derived from AFM in tapping mode is shown in Fig. 3. Atomic force micrographs suggested that only few lateral associations occur between adjacent nanofibres. Nanofibres are much more clearly defined probably because of the removal of pectic polysaccharides. The nanofibres obtained (69% yield) after the efficient mechanism of reduction in size (to submicron level) of acid treated PALF fibers seem to be more interwoven and their diameters were estimated between 5 and 15 nm as shown in Fig. 3. Thus the nanocellulose isolated from pineapple leaf fibre (PALF) has various characteristics desired for biomedical applications, such as high cross-linking, uncomplicated chemical structure and non-toxic. For biomedical applications, physical cross-linking has the advantages of not leaving residual amounts of the toxic cross-linking agent. Due to its unique nanostructure and properties, PALF nanocellulose is a natural candidate for numerous medical and tissue-engineered applications since it is both durable and biocompatible. The non-woven ribbons of nanocellulose closely resemble the structure of microbial cellulose (Iguchi, Yamanaka, & Budhiono, 2000; Klemm, Shumann, Udhardt, & Marsch, 2001) and native extracellular matrices, suggesting that it could function as a scaffold for the production of many tissue-engineered constructs.

The morphology of the nanocomposite was studied by ESEM (Fig. 4). Cellulose nanofibrils, approximately 15 nm in diameter and with the considerable aspect ratio, are apparent and well dispersed in the polyurethane matrix. No large aggregates and a homogeneous distribution of the nanofibres in the PU matrix were observed in the nanocomposite micrograph, implying good adhesion between fillers and matrix. This should be attributed to the hydrophilicity of both nanocellulose and polyurethane and the hydrogen-bonding interactions existing in filler/filler and filler/matrix, where the hydroxyl (–O–H) group of nanocellulose can interact with the carbonyl (>C=O) group of the polyurethane matrix (Scheme 1). Thus an even and uniform distribution of the nanocellulose in the polyurethane matrix is feasible, which could play an important role in improving the mechanical performance of the resulting nanocomposite.

After preparation of cellulose nanocomposites, it was essential to confirm that the cellulose nanofibrils in the prepared composites preserves cellulose I structure. The X-ray diffraction (XRD) spectra for nanocellulose (NC) and the nanocomposite with nanocellulose content of 5 wt% [PU–NC(5%)] are presented in Fig. 5. The peak at 22.7° is characteristic of cellulose I (Wada, Sugiyama, & Okano, 1993). Despite low cellulose content, the peak is clearly visible also in PU–NC(5%). This provides additional evidence that the original crystalline structure of cellulose (cellulose I) is still present in the nanocomposite. Most likely, nanofibril surfaces and disordered regions are swollen, without any influence on the interior of crystalline regions.

The nanocomposites prepared for uniaxial tensile tests contained 2, 5, and 10 wt% of nanocellulose and were termed PU–NC(2%), PU–NC(5%) and PU–NC(10%). Typical stress–strain

Scheme 1. Interaction between polyurethane and cellulose fibers.

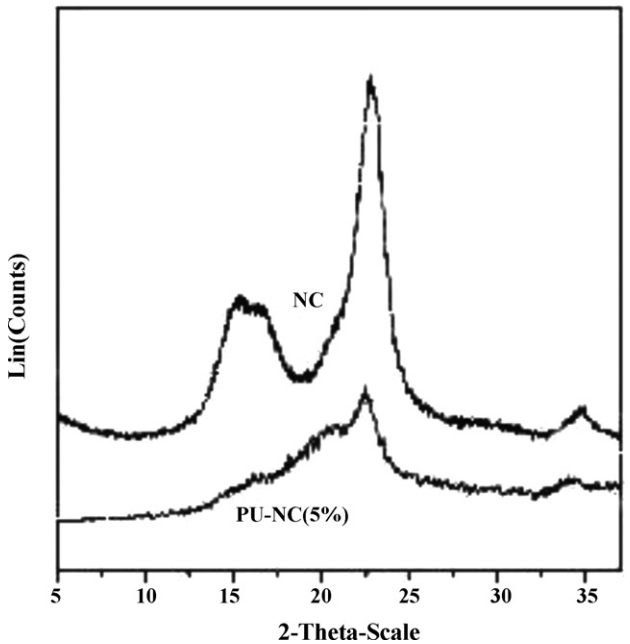

Fig. 5. XRD patterns of nanocellulose (NC) and polyurethane–nanocellulose (5%) nanocomposite.

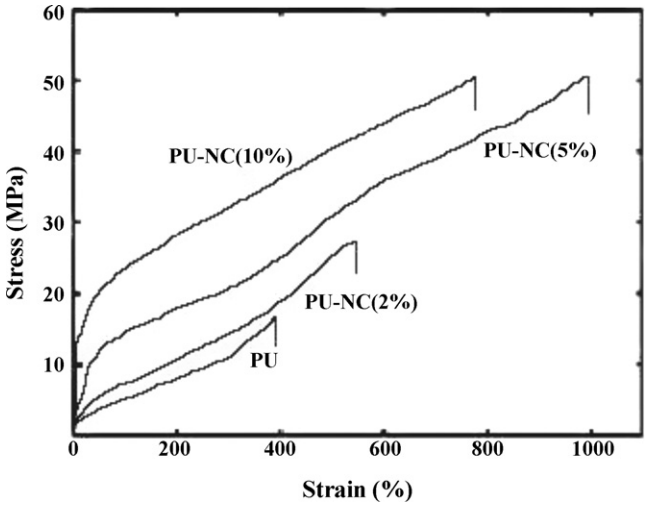

Fig. 6. Stress–strain curves for polyurethane (PU) and polyurethane–nanocellulose (PU–NC) composites.

curves are shown in Fig. 6. The data for tensile strength and strain-to-failure are summarized in Table 1.

The mechanical properties of neat polyurethane and nanocellulose–polyurethane composites are shown in Table 1.

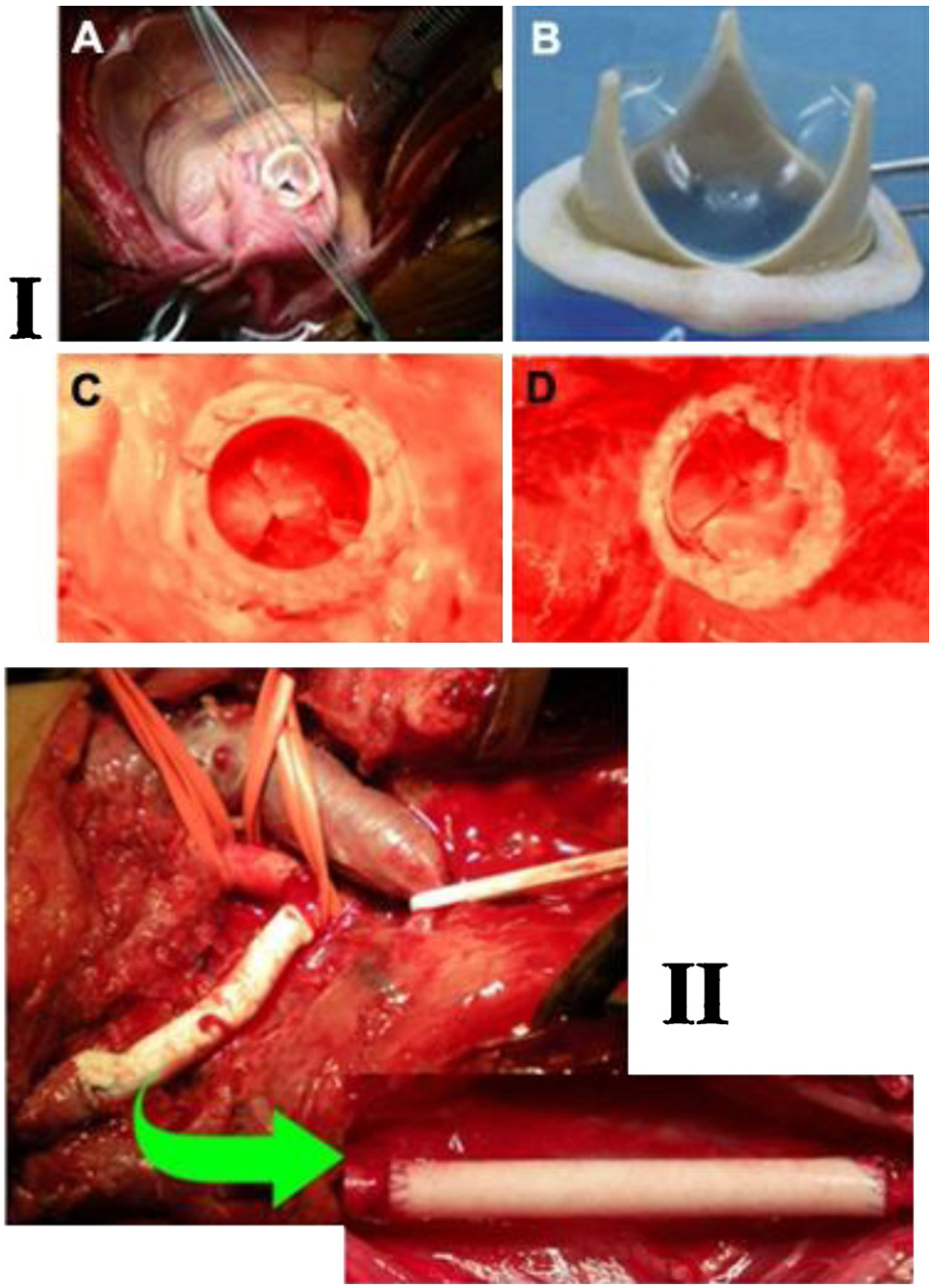

Fig. 7. (I) Nanocellulose–polyurethane prosthetic heart valve: (A) valve implant, (B) heart valve, (C) viewed in situ immediately prior to explant (inflow surface), (D) viewed in situ immediately prior to explant (outflow surface). (II) Vascular prostheses made of nanocellulose-polyurethane placed between the brachiocephalic trunk and the right common carotid artery in a 26-year-old male patient with multiple endocrine neoplasia 2B (MEN 2B).

Table 1
Mechanical properties of pure polyurethane and cellulose embedded composites.

Sample	Tensile strength (MPa)	E-modulus (MPa)
PU	17.5 ± 0.4	37.5 ± 0.5
PU–NC(2%)	28.2 ± 1.2	94 ± 1.6
PU–NC(5%)	52.6 ± 0.7	992.4 ± 1.9
PU–NC(10%)	51.3 ± 0.1	786.8 ± 1.4

The results show that the mechanical properties of composites were improved with an increase in nanocellulose content. The increase in the tensile strength was significant, which supports the hypothesis that polyurethane and cellulose are compatible as they are both hydrophilic. The strength of the PU–NC(2%) was increased by 160% compared with neat PU. The addition of 5 wt% nanocellulose in PU matrix also increased the E-modulus value by more than 2600% and the higher fibre content (10 wt%) increased it by almost 2100%. Table 1 shows the mechanical properties of the nanocomposites. The nanofibril proves to be more effective reinforcement in the polyurethane matrix offering high strength. The strength was improved from 17.5 MPa for neat PU to 52.6 MPa (almost 300%) for the PU–NC(5%) composite, and the modulus was improved from 37.5 to 992.4 MPa, which is almost 2600% higher. These results clearly show the high compatibility of nano size reinforcement in the polyurethane. The cellulose nanofibrils will integrate within the polymer matrix much better due to the

smaller size but this great improvement is also expected due to better reinforcing ability of high cross-linked nanofibrils network of cellulose in the prepared nanocomposites offering maximum reinforcement. The increase of the probability of the cellulose linkages can be observed at the nano-scale. The optimal increase in properties is exhibited for PU–NC(5%) nanocomposite, which is expected due to the well distribution of the filler particles inside the matrix.

3.2. Medical applications of developed nano-biocomposite of polyurethane

3.2.1. Heart valve

Continuing advances in prosthetic heart valve design and techniques for their implantation have improved the survival time and quality of life for patients who receive these devices.

In an ongoing effort to develop more durable and compatible heart valve prostheses, researchers have used a variety of techniques to determine the suitability of given valve materials for a given implant application. This suitability is generally known as "biocompatibility". Researchers commonly deal with biocompatibility in terms of whether the implant material or its degradation products, if any, initiate adverse tissue responses in the host, or conversely, whether deleterious changes in the chemical, physical, or mechanical properties of the implant material are caused by the host environment. The term "hemocompatibility" refers more specifically to biocompatibility issues related to implantation of prosthetic devices (such as prosthetic heart valves and vascular or coronary stents) in the cardiovascular system, such as any toxicity of implanted materials to red blood cells or tissues contacted by the implanted material, thrombosis, and induction of mineralization. The vast majority of biocompatibility studies to date have involved in vitro testing or animal models. However, the ultimate test for biocompatibility of a material, device, or prosthesis is human implantation.

To be clinically effective, a heart valve must endure a difficult environment, including cyclic bending stresses on the leaflets and high pressure transients across the valve, for long periods of time. Prosthetic heart valves currently in clinical use are of two general varieties: mechanical or tissue. Mechanical heart valves are very durable, but their use is complicated by higher risks of thromboembolism, hemorrhage, and hemolysis. Use of mechanical heart valves suffers the further complication of requiring chronic systemic anticoagulation of the patient. Tissue valves require no chronic anticoagulation, on the other hand, but often fail in a far shorter period of time than mechanical valves due to mineralization (the formation of mineral deposits, e.g. calcium phosphates) and tissue tearing. Potential alternative materials that are sufficiently durable and blood compatible for use in a prosthetic heart valve include bio polymers, such as cellulose polyurethanes, which can be effectively showing less mineralization than glutaraldehyde-fixed bovine pericardial tissue.

The development of PALF nanocellulose–polyurethane valve design [Fig. 7(I)] with good biological durability, fatigue resistance and haemodynamics, and a new generation of biostable polyurethanes which have proven themselves of superior biostability in a demanding 6-month, strained, rat implant model. Thus anticipate early development of a polyurethane valve which has a good haemodynamic function maintained during long-term implant, and which neither fails from biological degradation nor from fatigue-induced material failure, while maintaining a low thrombogenic surface. In accelerated fatigue tests, five out of five consecutively produced valves exceeded the equivalent of 12 years cycling without failure. The only failure occurred after the equivalent of approximately 13 years cycling, and three valves have reached 608 million cycles (approximately 15 years equivalent) to date.

3.2.2. Vascular grafts

Atherosclerotic cardiovascular disease is the number one cause of morbidity and mortality in the western world. This type of disease produces localized reduction in the calibre of arteries (stenosis) which ultimately leads to occlusion. It reduces or even stops the flow of blood through affected vessels. When this occurs, the overall consequences range from gangrene to stroke or to myocardial infarction.

Vascular bypass is one modality effective in the treatment of ischemic syndromes secondary to impeded blood flow. In the low flow small vessel setting, such as the coronary arteries and infrapopliteal vessels, the saphenous vein is the gold standard against which any prosthetic vascular conduit must compare. There is a significant number of cardiac and peripheral vascular cases in which the saphenous vein is either unsuitable (due to intrinsic disease such as sclerosis or varicosities), or is not available (due to stripping or previous vascular surgery). Another need exists in the area of hemodialysis for patients end-stage renal disease. In such a setting, the need for an off-the-shelf arterial blood vessel substitute is vital.

PALF derived nanocellulose embedded Polyurethane has been utilized as an attractive and readily available range of materials for the fabrication of vascular Prostheses. The elastic properties of the material, coupled with low thrombogenicity and exceptional physical and mechanical properties, has led to a considerable research effort aimed at the development of nanocellulose polyurethane vascular grafts [Fig. 7(II)]. Nanocellulose–PU vascular grafts with a wall thickness of 0.7–1.0 mm showed elongation at break of 800–1200%, and withstood hydraulic pressures up to 300 kPa.

4. Conclusions

This study has been concerned how the degree of individualization affects the PALF fibre morphology from the micro to the nanoscale. The steam explosion process resulted in PALF nanofibres having a width in the range of 5–15 nm. The used chemical treatments resulted in the individualized PALF microfibres and further steam treatment formed a network structure of PALF nanofibres. The high pressure defibrillation contributed a unique morphology of the interconnected web-like structure of nanofibres. Percentage yield and aspect ratio of the nanofiber obtained by this technique is observed to be very high in comparison with other conventional methods. High tensile strength and high strain-to-failure nanocomposites with strongly improved modulus were synthesized based on nanocellulose and polyurethane. The cellulose nanocomposites were prepared by solvent casting, based on dry crystalline cellulose and hydrophilic polyurethane. Cellulose dissolution was avoided while still allowing successful dispersion of the cellulose nanofibrils present in dry nanoscale cellulose particles. ESEM proves the presence of dispersed cellulose nanofibrils in the developed nanocomposites. The XRD analysis confirms that cellulose nanofibrils in the prepared nanocomposites preserves the original crystalline structure of cellulose (cellulose I). The composition with 5 wt% cellulose was optimal and showed the highest strain-to-failure. The produced nanocellulose and its composites confirmed to be a very versatile material having the wide range of medical applications, including cardiovascular implants, scaffolds for tissue engineering, repair of articular cartilage, vascular grafts, urethral catheters, mammary prostheses, penile prostheses, adhesion barriers and artificial skin. These implants were produced from bioresorbable and/or biodegradable materials. Progressive degradation of the implant material may

then be accompanied by the formation of the new tissues. The developed material can also be utilized for construction of non latex condoms, breathable wound dressing, surgical gloves, surgical gowns or drapes, medical bags, organ retrieval bags and medical disposables.

References

Alves, C., Ferrão, P. M. C., Silva, A. J., Reis, L. G., Freitas, M., Rodrigues, L. B., et al. (2010). Ecodesign of automotive components making use of natural jute fiber composites. *Journal of Cleaner Production*, *18*, 313–327.

Arib, R. M. N., Sapuan, S. M., Ahmad, M. M. H. M., Paridah, M. T., & Zaman, H. M. D. K. (2006). Mechanical properties of pineapple leaf fibre reinforced polypropylene composites. *Materials & Design*, *27*, 391–396.

Atalla, R. H., & Vanderhart, D. L. (1984). Native cellulose: A composite of two distinct crystalline forms. *Science*, *223*, 283–285.

Auad, M. L., Contos, V. S., Nutt, S., Aranguren, M. I., & Marcovich, N. E. (2005). Proceedings of COMAT 2005. *Polyurethane reinforced with nano/micro sized cellulose fibers*, 35–36.

Avellar, B. K., & Glasser, W. G. (1998). Steam-assisted biomass fractionation. I. Process considerations and economic evaluation. *Biomass and Bioenergy*, *14*, 205–218.

Bengtsson, M., Gatenholm, P., & Oksman, K. (2005). The effect of cross-linking on the properties of polyethylene/wood flour composites. *Composites Science and Technology*, *65*, 1468–1479.

Chakraborty, A., Sain, M., & Kortschot, M. (2006). Cellulose microfibers as reinforcing agents for structural materials. In K. Oksman, & M. Sain (Eds.), *Cellulose nanocomposites: Processing, characterization, and properties* (pp. 169–186). ACS Symposium Series.

Cherian, B. M., Leão, A. L., de Souza, S. F., Thomas, S., Pothan, L. A., & Kottaisamy, M. (2010). Isolation of nanocellulose from pineapple leaf fibres by steam explosion. *Carbohydrate Polymers*, *81*, 720–725.

De Souza Lima, M., & Borsali, R. (2004). Rodlike cellulose microcrystals: Structure, properties, and applications. *Macromolecular Rapid Communications*, *25*, 771–787.

Dufresne, A., & Vignon, M. (1998). Improvement of starch film performances using cellulose microfibrils. *Macromolecules*, *31*, 2693–2696.

Gorrasi, G., Tortora, M., & Vittoria, V. (2005). Synthesis and physical properties of layered silicates/polyurethane nanocomposites. *Journal of Polymer Science Part B: Polymer Physics*, *43*, 2454–2467.

Iguchi, M., Yamanaka, S., & Budhiono, A. (2000). Bacterial cellulose – A masterpiece of nature's arts. *Journal of Materials Science*, *35*, 261–270.

Jacob, M., Francis, B., Varughese, K. T., & Thomas, S. (2006). The effect of silane coupling agents on the viscoelastic properties of rubber biocomposites. *Macromolecular Materials and Engineering*, *291*, 1119–1126.

Jacob, M., Varughese, K. T., & Thomas, S. (2006). Dielectric characteristics of sisal–oil palm hybrid biofibre reinforced natural rubber biocomposites. *Journal of Materials Science*, *41*, 5538–5547.

Jacob, M., Jose, J., Jose, S., Varughese, K. T., & Thomas, S. (2010). Viscoelastic and thermal properties of woven-sisal-fabric-reinforced natural-rubber biocomposites. *Journal of Applied Polymer Science*, *117*, 614–621.

John, M. J., & Anandjiwala, R. D. (2009). Chemical modification of flax reinforced polypropylene composites. *Composites Part A: Applied Science and Manufacturing*, *40*, 442–448.

John, M. J., & Thomas, S. (2008). Biofibres and biocomposites. *Carbohydrate Polymers*, *71*, 343–364.

John, M. J., Anandjiwala, R. D., Pothan, L. A., & Thomas, S. (2007). Cellulosic fibre reinforced green composites. *Composite Interfaces*, *14*, 733–751.

Khadem, H. S. (1988). *Carbohydrate chemistry: Monosaccharides and their oligomers*. Academic Press: New York.

Kim, S. J., Moon, J. B., Kim, G. H., & Ha, C. S. (2008). Mechanical properties of polypropylene/natural fiber composites: Comparison of wood fiber and cotton fiber. *Polymer Testing*, *27*, 801–806.

Klemm, D., Philipp, B., Heinze, T., Heinze, U., & Wagenknecht, W. (1998). Comprehensive cellulose chemistry: Functionalization of cellulose. In D. Klemm, B. Philipp, T. Heinze, U. Heinze, & W. Wagenknecht (Eds.), *Comprehensive cellulose chemistry* (pp. 37–38). New York: Wiley-VCH.

Klemm, D., Shumann, D., Udhardt, U., & Marsch, S. (2001). Bacterial synthesized cellulose—Artificial blood vessels for microsurgery. *Progress in Polymer Science*, *26*, 1561–1603.

Kroonbatenburg, L. M. J., Kroon, J., & Northolt, M. G. (1986). Chain modulus and intramolecular hydrogen bonding in native and regenerated cellulose fibers. *Polymer Communications*, *27*, 290–292.

Lopattananon, N., Panawarangkul, K., Sahakaro, K., & Ellis, B. (2006). Performance of pineapple leaf fiber–natural rubber composites: The effect of fiber surface treatments. *Journal of Applied Polymer Science*, *102*, 1974–1984.

Moon, S. Y., Kim, J. K., Nah, C., & Lee, Y. S. (2004). Polyurethane/montmorillonite nanocomposites prepared from crystalline polyols, using 1,4-butanediol and organoclay hybrid as chain extenders. *European Polymer Journal*, *40*, 1615–1621.

Nakagaito, A. N., & Yano, H. (2005). Novel high-strength biocomposites based on microfibrillated cellulose having nano-order-unit web-like network structure. *Applied Physics A: Materials Science & Processing*, *80*, 155–159.

Nishiyama, Y., Langan, P., & Chanzy, H. (2002). Crystal structure and hydrogen-bonding system in cellulose Iβ from synchrotron X-ray and neutron fiber diffraction. *Journal of the American Chemical Society*, *124*, 9074–9082.

Nishiyama, Y., Sugiyama, J., Chanzy, H., & Langan, P. (2003). Crystal structure and hydrogen bonding system in cellulose Iα from synchrotron X-ray and neutron fiber diffraction. *Journal of the American Chemical Society*, *125*, 14300–14306.

Placet, V. (2009). Characterization of the thermo-mechanical behaviour of Hemp fibres intended for the manufacturing of high performance composites. *Composites Part A: Applied Science and Manufacturing*, *40*, 1111–1118.

Pothan, L. A., Cherian, B. M., Anandakutty, B., & Thomas, S. (2007). Effect of layering pattern on the water absorption behavior of banana glass hybrid composites. *Journal of Applied Polymer Science*, *105*, 2540–2548.

Rials, T. G., Wolcott, M. P., & Nassar, J. M. (2001). Interfacial contributions in lignocellulosic fiber-reinforced polyurethane composites. *Journal of Applied Polymer Science*, *80*, 546–555.

Samir, M. A. S. A., Alloin, F., & Dufresne, A. (2005). Review of recent research into cellulosic whiskers, their properties and their application in nanocomposite field. *Biomacromolecules*, *6*, 612–626.

Sternitzke, M., Derby, B., & Brook, R. J. (1998). Alumina/silicon carbide nanocomposites by hybrid polymer/powder processing: Microstructures and mechanical properties. *Journal of the American Ceramic Society*, *81*, 41–48.

Vaia, R. A. (2002). Polymer Nanocomposites open a new dimension for plastics and composites. *The AMPTIAC Newsletter*, *6*, 17–24.

Wada, M., Sugiyama, J., & Okano, T. (1993). Native celluloses on the basis of two crystalline phase (Iα/Iβ) system. *Journal of Applied Polymer Science*, *49*, 1491–1496.